Chapter 16
Biomedical Data Processing Using HHT: A Review

Ming-Chya Wu and Norden E. Huang

Abstract Living organisms adapt and function in an ever changing environment. Even under basal conditions they are constantly perturbed by external stimuli. Therefore, biological processes are all non-stationary and highly nonlinear. Thus the study of biomedical processes, which are heavily depending on observations, is crucially dependent on the data analysis. The newly developed method, the Hilbert-Huang Transform (HHT), is ideally suited for nonlinear and non-stationary data analysis such as appeared in the biomedical processes. Different from all other data analysis existing methods, this method is totally adaptive: It derives the basis from the data and based on the data. As a result, it is highly efficient in expanding any time series in their intrinsic modes, which reveal their full physical meaning. In this article, we review biomedical data processing by using HHT. We introduce two exemplary studies: cardiorespiratory synchronization and human ventricular fibrillation. The power and advantages of HHT are apparent from the achievements of these studies.

16.1 Introduction

Physiological systems are complex and their dynamical properties and the underlying biomedical processes can only be studied through some physicological and pathological data. The adaptation and the interactions and feedbacks amongst our body systems, however, make the physiological and pathological signals highly nonlinear and nonstationary [1]; consequently, the resultant biomedical signals are among the most complicated data there is. Since the underlying dynamics can only be studied through limited data, data analysis methods play a crucial role in the outcome. An essential task to analyze biomedical data is to extract essential component(s) that will be fully representative of the underlying biological

M.-C. Wu (✉)
Research Center for Adaptive Data Analysis, Department of Physics and National Central University, Chungli 32001, Taiwan; Institute of Physics, Academia Sinica, Nankang Taipei 11529, Taiwan
e-mail: mcwu@ncu.edu.tw

A. Nait-Ali (ed.), *Advanced Biosignal Processing*,
DOI 10.1007/978-3-540-89506-0_16, © Springer-Verlag Berlin Heidelberg 2009

processes. For this purpose, there should be criteria derived from the data itself to judge what is the inherent dynamics and what are the contributions of external factors and noises in the data. To accommodating the variety of complicated data, analysis method would then have to be adaptive. Here, adaptivity means that the definition of the basis has to base on and be derived from the data. Unfortunately, most currently available data analysis methods are based an a priori basis (such as trigonometric functions in Fourier analysis, for example); they are not adaptive [2]. From the viewpoint of data analysis, the ultimate goal is not to find the mathematical properties of data, but is to uncover the physical insights and implications hidden in the data. There are no a priori reasons to believe that a basis functional, however cleverly designed, is capable of representing the variety of the underlying physical processes. An a posteriori adaptive basis provides a totally different approach from the established mathematical paradigm; though it may also present a great challenge to the mathematical community.

The recently developed Empirical Mode Decomposition (EMD) and the associated Hilbert Spectral Analysis (HSA), together designated as the Hilbert-Huang Transform (HHT) [2], represents such a paradigm shift of data analysis methodology. The HHT is designed specifically for analyzing data from nonlinear and nonstationary processes. From the very beginning, HHT had been proved to be a powerful tool for biomedical data analysis in research [3–6].

The EMD uses the sifting process to extract monocomponent signal by eliminating riding waves and making the wave-profiles more symmetric. The expansion of any data set via the EMD method has only a finite-number of locally non-overlapping time scale components, known as Intrinsic Mode Functions (IMFs) [2]. Each intrinsic mode, linear or nonlinear, represents a simple oscillation, which has the same number of extrema and zero-crossing. In comparison with simple har-

Table 16.1 Comparison between Fourier, wavelet, and HHT analysis. Adapted from Ref. [7]

	Fourier	Wavelet	HHT
Basis	a priori	a priori	a posteriori, Adaptive
Frequency	Integral transform over global domain, Uncertainty	Integral transform over global domain, Uncertainty	Differentiation over local domain, Certainty
Presentation	Energy in frequency space	Energy in time-frequency space	Energy in time-frequency space
Nonlinearity	No	no	Yes
Nonstationarity	No	yes	Yes
Feature Extraction	No	Discrete: no Continuous: yes	Yes
Theoretical base	Complete mathematical theory	Complete mathematical theory	Empirical

monic functions, the IMF can have a variable amplitude and frequency as functions of time. Furthermore, these IMFs as bases are complete and orthogonal to each other. All IMFs enjoy good Hilbert transform such that they are suitable for spectral analysis. The adaptive properties of HHT to empirical data further make it easy to give physical significations to IMFs. Table 16.1 summarizes comparisons between Fourier, wavelet, and HHT analysis [7].

The power and effectiveness of HHT in data analysis have been demonstrated by its successful applications to many important problems covering engineering, biomedical, financial and geophysical data. Recently, 2 dimensional version of HHT [8–12] has also been developed and applied to image processing. Readers interested in completed details can consult Refs. [2, 7] and Refs. [9–12]. In this article, we review biomedical data processing by using 1D HHT. Due to the limit of space, here we focus on two exemplary studies: cardiorespiratory synchronization (CS) [13–15], and human ventricular fibrillation (VF) [16, 17]. From the outcome of these studies, the advantages and power of HHT are apparent.

16.2 Empirical Mode Decomposition

The EMD in HHT is developed on the assumption that any time series consists of simple intrinsic modes of oscillations, and the essence of the method is to identify the intrinsic oscillatory modes by their characteristic time scales in the data empirically and then decompose the data accordingly [2]. The resultant components decomposed from the EMD are IMFs, which are symmetric with respect to the local mean and have the same numbers of zero crossings and extremes. This is achieved by sifting data to generate IMFs. The algorithm to create IMFs in the EMD consists of two main steps [2]:

Step-1: Identify local extrema in the experimental data $x(t)$. All the local maxima are connected by a cubic spline line $U(t)$, which forms the upper envelope of the data. Repeat the same procedure for the local minima to produce the lower envelope $L(t)$. Both envelopes will cover all the data between them. The mean of upper envelope and lower envelope $m_1(t)$ is given by:

$$m_1(t) = \frac{U(t) + L(t)}{2} \tag{16.1}$$

Subtracting the running mean $m_1(t)$ from the original time series $x(t)$, we get the first component $h_1(t)$,

$$h_1(t) = x(t) - m_1(t) \tag{16.2}$$

The resulting component $h_1(t)$ is an IMF if it is symmetric and has all maxima positive and all minima negative. An additional condition of intermittence can be imposed here to sift out waveforms with certain range of intermittence for physical consideration. If $h_1(t)$ is not an IMF, the sifting process has to be repeated as many times as it is required to reduce the extracted signal to an IMF. In the subsequent

sifting process steps, $h_1(t)$ is treated as the data to repeat above steps mentioned above,

$$h_{11}(t) = h_1(t) - m_{11}(t) \tag{16.3}$$

Again, if the function $h_{11}(t)$ does not yet satisfy criteria for IMF, the sifting process continues up to k times until some acceptable tolerance is reached:

$$h_{1k}(t) = h_{1(k-1)}(t) - m_{1k}(t) \tag{16.4}$$

Step-2: If the resulting time series is an IMF, it is designated as $c_1 = h_{1k}(t)$. The first IMF is then subtracted from the original data, and the difference r_1 given by

$$r_1(t) = x(t) - c_1(t) \tag{16.5}$$

is the residue. The residue $r_1(t)$ is taken as the original data, and we apply to it again the sifting process of *Step-1*.

Following the procedures of *Step-1* and *Step-2*, we continue the process to find more intrinsic modes c_i until the last one. The final residue will be a constant or a monotonic function which represents the general trend of the time series. Finally, we obtain

$$x(t) = \sum_{i=1}^{n} c_i(t) + r_n \tag{16.6}$$

$$r_{i-1}(t) - c_i(t) = r_i(t) \tag{16.7}$$

Here we remark that an extended version of EMD, named Ensemble EMD (EEMD) [18], has recently been developed to improve the mode-mixing problem which may occur in EMD and makes each component lack of full physical meaning. The EEMD is implemented by constructing a sufficiently large amount of realizations each combines $x(t)$ and a white noise, and taking average for the IMFs decomposed by EMD from these realizations. By using the fact that average of large amount of white noise converges to null, the noise has zero net effect on the data but is beneficial to effective sifting in decomposition. It has been shown that EEMD indeed performs better than the primary version of EMD from avoiding the mode mixing problem. Since EMD and EEMD are essentially in the same framework, here we only discuss EMD. Details of EEMD can be found in Ref. [18].

The instantaneous phase of IMF can be calculated by applying the Hilbert transform to each IMF, say the rth component $c_r(t)$. The procedures of the Hilbert transform consist of calculation of the conjugate pair of $c_r(t)$, i.e.,

$$y_r(t) = \frac{1}{\pi} P \int_{-\infty}^{\infty} \frac{c_r(t')}{t - t'} dt' \tag{16.8}$$

where P indicates the Cauchy principal value. With this definition, two functions $c_r(t)$ and $y_r(t)$ forming a complex conjugate pair, define an analytic signal $z_r(t)$:

$$z_r(t) = c_r(t) + iy_r(t) \equiv A_r(t)e^{i\phi_r(t)} \tag{16.9}$$

with amplitude $A_r(t)$ and instantaneous phase $\phi_r(t)$ defined by

$$A_r(t) = [c_r^2(t) + y_r^2(t)]^{1/2} \tag{16.10}$$

$$\phi_r(t) = \tan^{-1}\left(\frac{y_r(t)}{c_r(t)}\right) \tag{16.11}$$

Then, one can calculate the instantaneous phase from Eqs. (16.8) and (16.11).

16.3 Cardiorespiratory Synchronization

First, we present an application of HHT to the study of CS [13, 14, 15]. CS is a phenomenon originating from the interactions between cardiovascular and the respiratory systems. The interactions can lead to a perfect locking of their phases whereas their amplitudes remain chaotic and non-correlated [19]. The nature of the interactions has been extensively studied in recent years [20–42]. Recently, Schäfer et al. [32, 33] and Rosenblum et al. [34] applied the concept of phase synchronization of chaotic oscillators [43] to analyze irregular non-stationary bivariate data from cardiovascular and respiratory systems, and introduced the cardiorespiratory synchrogram (CRS) to detect different synchronous states and transitions between them. They found that there were sufficiently long periods of hidden synchronization and concluded that the CS and respiratory sinus arrhythmia (RSA) are two competing factors in cardiorespiratory interactions. Since then, CS has been reported in young healthy athletes [32, 33], healthy adults [34–36], heart transplant patients [34], infants [38], and anesthetized rats [39]. More recently, Kotani et al. [40] further developed a physiologically model from these observations to study the phenomena, and showed that both the influence of respiration on heartbeat and the influence of heartbeat on respiration are important for CS. Since aforementioned studies are mostly based on measured data, the data processing method plays a crucial role in the outcome. The essential part of such investigations is the extraction of respiratory rhythms from noisy respiratory signals. A technical problem in the analysis of the respiratory signal then arises: insufficiently filtered signals may still have too many noises, and over-filtered signal may be too regular to lose the characteristics of respiratory rhythms: Improper analysis methods may lead to misleading results.

To overcome these difficulties, Wu and Hu [13] proposed using the EMD for such studies and got significantly reasonable results. Unlike conventional filters, the EMD provides an effective way to extract respiratory rhythms from experimental respiratory signals. The adaptive properties of EMD to empirical data make it

easy to give physical significations to IMFs, and allow one to choose a certain IMF as a respiratory rhythm [13]. In the implement of EMD, respiratory rhythms are extracted from empirical data by using the number of respiratory cycles per minute for human beings as a criterion in the sifting process of EMD [13]. They considered empirical data consisting of 20 data sets which were collected by the Harvard medical school in 1994 [44]. Ten young (21–34 years old) and ten elderly (68–81 years old) rigorously-screened healthy subjects underwent 120 minutes of continuous supine resting while continuous electrocardiogram (ECG) and respiration signals were collected. The continuous ECG and respiration data were digitized at 250 Hz (respiratory signals were later preprocessed to be at 5 Hz). Each heartbeat was annotated using an automated arrhythmia detection algorithm, and each beat annotation was verified by visual inspection. Each group of subjects includes equal numbers of men and women. In the following, we will review the scheme proposed by Wu and Hu [13], and focus on the application of HHT to CS. Details of the study and extended investigations which are not included herein will be referred to the original paper [13].

The respiratory signals represent measures of the volume of expansion of ribcage, so the corresponding data are all positive numbers and there are no zero crossings. In addition to respiratory rhythms, the data also contain noises originating from measurements, external disturbances and other factors. From the EMD decomposition, one can select one component as the respiratory rhythm according to the criteria of intermittencies of IMFs imposed in *Step-1* as an additional sifting condition [13]. Among IMFs, the first IMF has the highest oscillatory frequency, and the relation of intermittence between different modes is roughly $\tau_n = 2^{n-1}\tau_1$ with τ_n the intermittence of the n th mode. The reason for such a dyadic intermittence criterion selection is that the EMD indeed represents a dyadic filter bank as suggested by Flandrin et al. [45] and Wu and Huang [46].

More explicitly, the procedures for the analysis are as follows [13]: (i) Apply the EMD to decompose the recorded data into a number of IMFs. Since the respiratory signal was preprocessed to a sampling rate of 5 Hz, there should be (10–30) data points in one respiratory cycle[1]. Thus, for example, one can use c_1: (3–6), c_2: (6–12), c_3: (12–24), . . . , etc. After the sifting processes of the EMD, the original respiratory data are decomposed into n IMFs $c_1, c_2, \ldots, c_n$, and a residue r_n. (ii) Visually inspect the resulting IMFs. If the amplitude of a certain mode is dominant and the waveform is well distributed, then the data are said to be well decomposed, and the decomposition is successfully completed. Otherwise, the decomposition may be inappropriate, and one has to repeat step (i) with different parameters.

Figure 16.1 shows the decomposition of an empirical signal with a criterion of the intermittence being (3–6) data points for c_1, and $(3 \times 2^{n-1} - 3 \times 2^n)$ data points for c_n's with $n > 1$. Comparing $x(t)$ with c_i's, it is obvious that c_3 preserves the

[1]The number of breathing per minute is about 18 for adults, and about 26 for children. For different healthy states, the number of respiratory cycles may vary case by case. To include most of these possibilities, respiratory cycles ranging from 10 to 30 times per minute were taken. Each respiratory cycle then roughly takes 2–6 s, i.e., (10–30) data points.

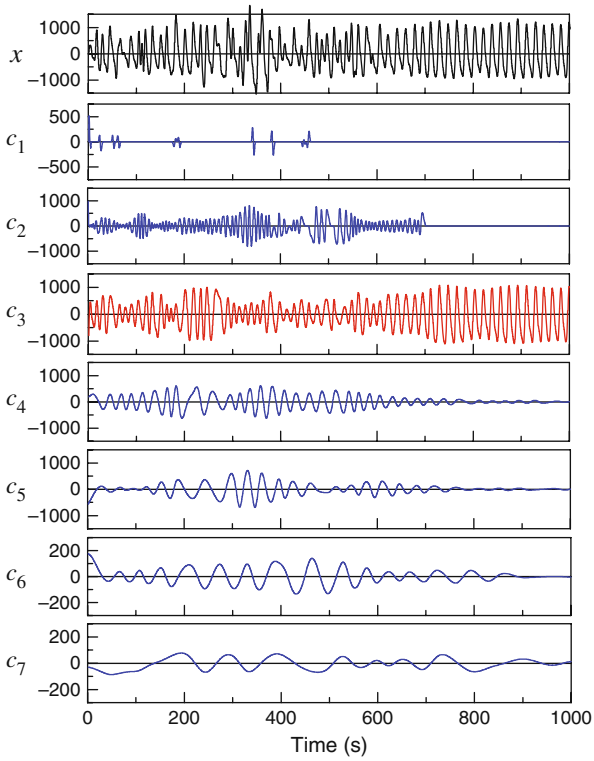

Fig. 16.1 Example of EMD for a typical respiratory time series (code f1o01 in the database [44]). The criterion for intermittence in the sifting process is (3–6) data points per cycle for c_1. Signal $x(t)$ is decomposed into 14 components including 13 IMFs and 1 residue; here, only the first 7 components are shown. After Ref. [13]

main structure of the signal and is also dominant in the decomposition. One can see that component c_3,with (12–24) data points per respiratory cycle, corresponds to the respiratory rhythm. Figure 16.2 compares respiratory signal in various stages. In Fig. 16.2a, a typical respiratory time series data $x(t)$ is shown. The preprocessed signal $x'(t)$ by a proper Fourier band filter is shown in Fig. 16.2b, in which only fast oscillatory noises are filtered out, and main structures of the signal are preserved. Figure 16.2c shows the IMF $c_3(t)$ obtained by performing EMD on $x'(t)$. The process is similar to that used to obtain $c_3(t)$ in Fig. 16.1. Obviously, IMF $c_3(t)$ of Fig. 16.2c still preserves characteristic structure of $x(t)$ shown in Fig. 16.2a. Here we should emphasize that the preprocessing to have $x'(t)$ is not necessary in the framework of EMD. We show $x'(t)$ only for comparison.

After selecting one IMF as the respiratory rhythm, one can proceed in the calculation of the instantaneous phase by the Hilbert transform and incorporating with heartbeat signals to construct CRS, which is a visual tool for inspecting synchronization. Let us denote the phase of the respiratory signal calculated by using Eq. (16.11) as ϕ_r and the heartbeat as ϕ_c. If the phases of respiratory signal $\phi_r$and heartbeat ϕ_c are coupled in a fashion that a cardiovascular system completes n heartbeats in m respiratory cycles, then a roughly fixed relation can be proposed. In general, there is a phase and frequency locking condition [13, 19, 32, 33].

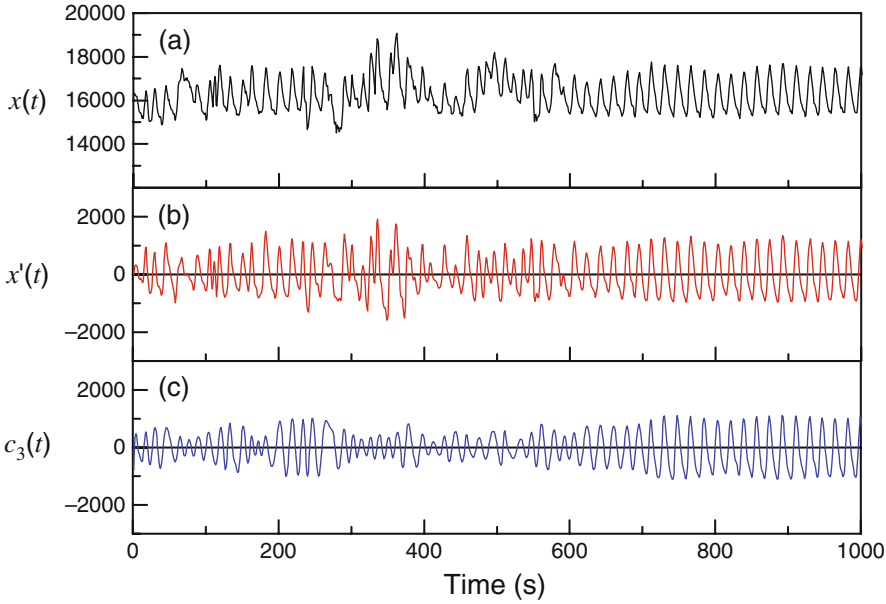

Fig. 16.2 Comparison of respiratory signals for a typical subject (code f1o01) in different data processing stages: (**a**) original experimental time series $x(t)$, (**b**) after performing low pass filtering, $x'(t)$, and (c) the third IMF $c_3(t)$ in Fig. 16.1, after performing EMD on $x'(t)$. Adapted from Ref. [13]

$$|m\phi_r - n\phi_c| \leq const \tag{16.12}$$

with m, n integer. According to Eq. (16.12), for the case that ECG completes n cycles while the respiration completes m cycles, it is said to be synchronization of n cardiac cycles with m respiratory cycles. Using the heartbeat event time t_k as the time frame, Eq. (16.12) implies the relation

$$\phi_r(t_{k+m}) - \phi_r(t_k) = 2\pi m \tag{16.13}$$

Furthermore, by defining

$$\Psi_m(t_k) = \frac{1}{2\pi}\,[\phi_r(t_k) \mod 2\pi m] \tag{16.14}$$

and plotting $\Psi_m(t_k)$ versus t_k, synchronization will result in n horizontal lines in case of $n:m$ synchronization. By choosing n adequately, a CRS can be developed for detecting CS [32, 33]. Example of 3:1 synchronization with $n = 6$ and $m = 2$ is shown in Fig. 16.3, where phase locking appear in several epochs, e.g., at 2800–3600 s, and there are also frequency locking, e.g., at 400 s, near which there are n parallel lines with the same positive slope.

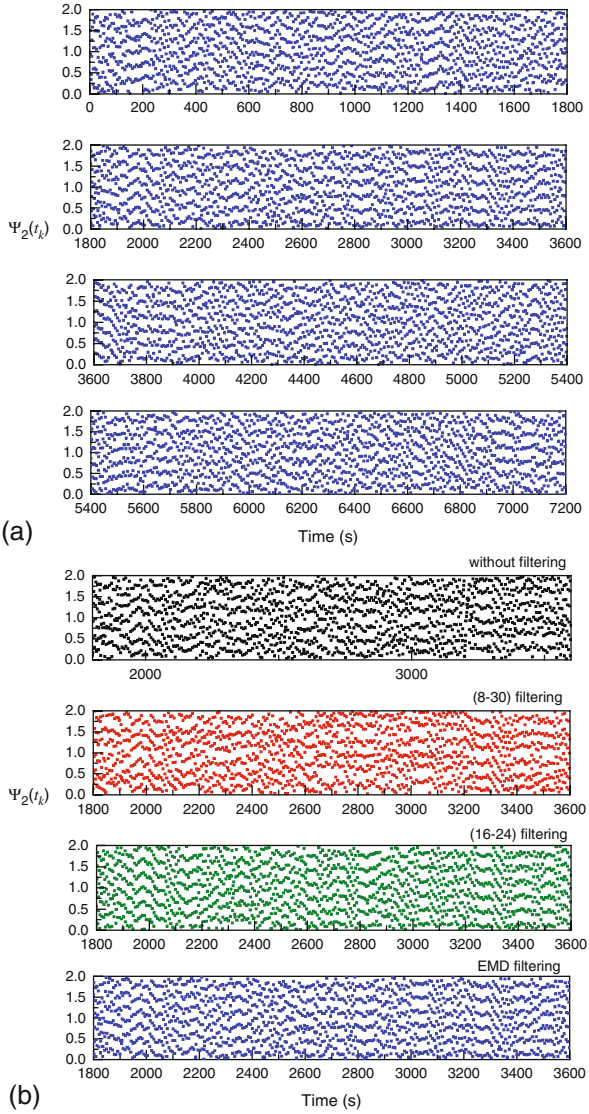

Fig. 16.3 CRS for a typical subject (code f1o06). (**a**) Empirical data are preprocessed by the EMD method. There are about 800 sec synchronization at 2800–3600 sec, and several spells of 50–300 sec at other time intervals. (**b**) Comparison of the results without filtering (top one), preprocessed by the standard filters with windows of (8–30) and (16–24) cycles per minute (the second and the third ones), and the EMD method (bottom one). After Ref. [13]

For comparison, the results of the same subject in 1800–3600s, but with respiratory signals without filtering, preprocessed by the standard filters and the EMD are shown in Fig. 16.3b. The windows of the standard filters are (8–30) and (16–24) cycles per minute. In general, some noise dressed signals can still show synchronization in some epochs but the HSA failed at some time intervals (e.g., around 3400–3600 s of the case without filtering), and over-filtered signals reveal too strong synchronization (filter with window of 16–24). In other words, global

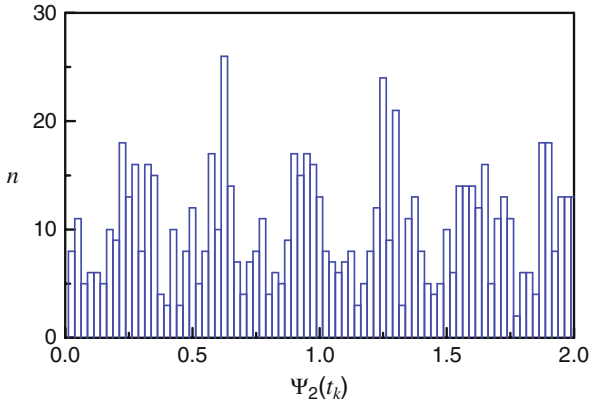

Fig. 16.4 Histogram of phase for the phase locking period from 2800 sec to 3600 sec for a typical subject (code f1o06) shown in Fig. 16.3a. After Ref. [13]

frequency used in standard filters may dissolve local structures of the empirical data. This does not happen in the EMD filtering.

Figure 16.4 shows the histogram of phases for the phase locking period from 2800 to 3600 s in Fig. 16.2a. Significant higher distribution can be found at $\Psi_2 \approx$ 0.25, 0.6, 0.9, 1.25, 1.6, 1.9 in the unit of 2π, indicating heartbeat events occur roughly at these respiratory phase during this period. Following above procedures, we analyze data of 20 subjects, and the results are summarized in Table 16.2. The results are ordered by the strength of CS. From our results, we do not find specific relations between the occurrence of synchronization and sex of the subjects as in Refs. [32, 33]. Here we note that if we use other filters to the same empirical data, we will have different results depending on the strength of synchronization. As noted above, data processing method plays a crucial role in the analysis of real data. Over-filtered respiratory signals may lose detailed structures and become too regular. It follows that final conclusions are methodological dependent.

To compare EMD and Fourier-based filter, we use the intermittency in the EMD analysis as the bandwidth of a generic Fourier-based filter to filter the same empirical data. We usually have different results depending on the strength of synchronization. For example, for the f1o06 subject, the intermittency of the third IMF is (12–24). Using (12–24) as a bandwidth of the generic Fourier-based filter, we have similar epochs of synchronization. However, for the f1y02 subject with intermittency of the second IMF (16–32) being selected to optimize the decomposition, we have more epochs of 3:1 synchronization lasting 50 s and new few 7:2 synchronization lasting 50 s and 80 s when the bandwidth of (16–32) is used. For the f1o05 subject in which the second IMF with intermittency (10–20) being selected, epochs of 5:2 synchronization lasting 50 s are found when the same bandwidth (10–20) is used. In comparison with the results presented in Table 16.2, the Fourier-based filter with a bandwidth of the same intermittency appears to smooth the data to have more regular wave form, and in turn usually have stronger synchronization. For a time series with variable intermittencies, the smoothing of data may introduce

Table 16.2 Summary of our results. 20 subjects are ordered by the strength (total time length) of CS. After Ref. [13]

Code	Sex	Age	Synchronization
flo06	F	74	3:1(800 s, 300 s, 250 s, 150 s, 100 s, 50 s)
f1y05	M	23	3:1(350 s, 300 s, 200 s, 100 s)
f1o03	M	73	3:1(200 s, 50 s, 30 s)
f1y10	F	21	7:2(200 s, 50 s), 4:1(50 s)
f1o07	M	68	7:2(120 s, 100 s, 80 s)
f1o02	F	73	3:1(100 s, several spells of 50 s)
f1y01	F	23	7:2(several spells of 30 s)
f1y04	M	31	5:2(80 s, 50 s, 30 s)
f1o08	F	73	3:1(50 s, 30 s)
f1y06	M	30	4:1(50 s, 30 s)
f1o01	F	77	7:2(several spells of 50 s)
f1y02	F	28	3:1(50 s)
f1y08	F	30	3:1(50 s)
f1o10	F	71	3:1(30 s)
f1o05	M	76	No synchronization detectable
f1y07	M	21	No synchronization detectable
f1y09	F	32	No synchronization detectable
f1y03	M	34	No synchronization detectable
f1o09	M	71	No synchronization detectable
f1o04	M	81	No synchronization detectable

additional modes which do not exist in some segments of the primary data and thus leads to misleading results. For example, in Fig. 16.5, comparisons for the results of the fly02 subject obtained by using the Fourier-based filter and the EMD approach are shown. The original time series $x(t)$ is dressed with noises such that the signal almost disappears at $t = 2320 - 2380$ sec. The Fourier-based filter introduces a new waveform at this epoch, but the new waveform having a local minimum larger than 0 can not be processed directly by the Hilbert transform. This is not the case for the waveform obtained from EMD method. Furthermore, at $t = 2000 - 2100$ sec, the Fourier-based filter does not preserve the structure of the original time series, and the waveform obtained from EMD is similar to the original time series. Therefore, from the aspect of data processing that could preserve the essential features of original empirical data, the EMD approach is better than Fourier based filtering.

From above investigation, we conclude that: (i) In most cases, cardiac oscillations are more regular than respiratory oscillations and the respiratory signal is the key factor for the strength of CS. (ii) Cardiorespiratory phase locking and frequency locking take place when respiratory oscillations become regular enough and have a particular frequency relation coupling with cardiac oscillations. Therefore, CS and RSA are competing factors [32, 33]. We observed the intermittence of respiratory oscillation varies with time but synchronization persists in some subjects. This confirms correlations in CS. (iii) Over-filtered respiratory signals may be too regular, and in turn, appear to have stronger synchronization than they shall have. As a result,

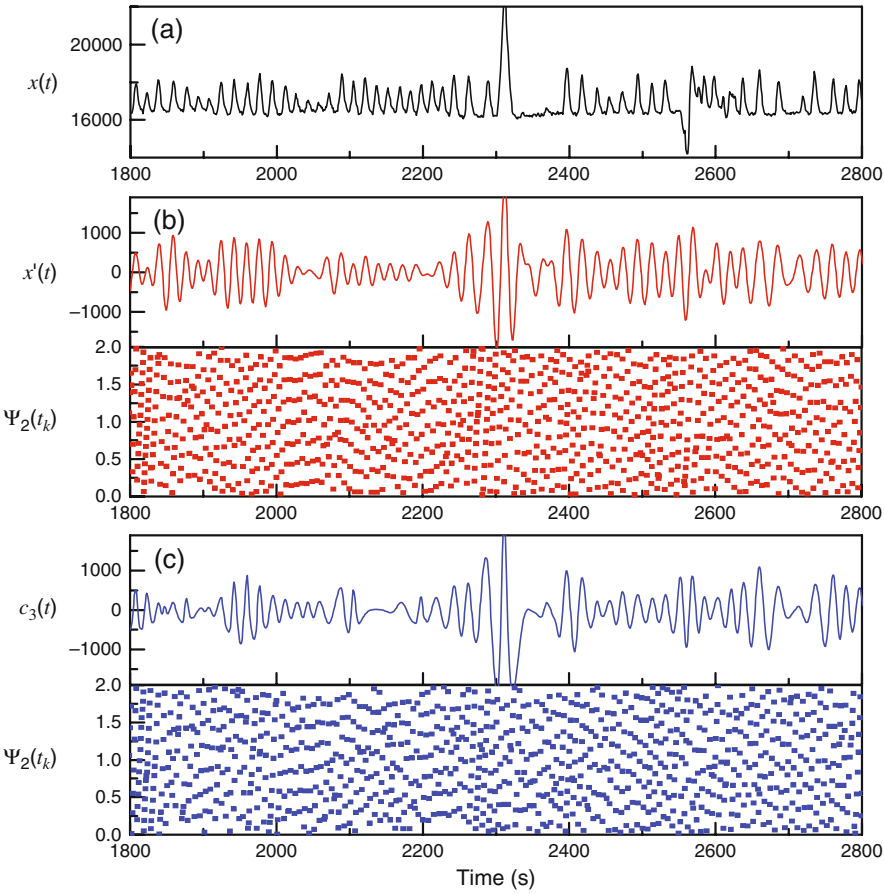

Fig. 16.5 Comparison of the data processing for a typical subject (code fly02). (**a**) The empirical time series, (**b**) the time series filtered by the Fourier-based filter with bandwidth (16–32) and the corresponding synchrogram, and (**c**) the time series of the third IMF decomposed by the EMD method with intermittency (16–32) and the corresponding synchrogram. After Ref. [13]

if the Fourier based approach with narrow band filtration is used, some epochs of phase locking or frequency locking should be considered as being originated from these effects.

16.4 Human Ventricular Fibrillation

Cardiac arrhythmias are disturbances in the normal rhythm, and fibrillation is manifested as irregular electrical activity of the heart. During fibrillation the coordinated contraction of the cardiac muscle is lost and the mechanical pumping effectiveness of the heart fails. Among these, ventricular fibrillation (VF) is known as the most

dangerous cardiac arrhythmia frequently leading to sudden cardiac death (SCD) [47]. Prediction of VF is thus an important issue in cardiology, yet to date; there exists no effective measure capable of predicting fatal VF. Since short-term VF can also occurs in the ECG of healthy people, the first task to this issue is to distinguish fatal VF from non-fatal VF.

Recently, Wu et al. [16, 17] investigated the empirical data of VF patients by using the approach of phase statistics to estimate the correlation between characteristic properties of VF ECG and the corresponding consequences, i.e., dead/alive outcome. They found that there is an explicit correlation which can be used as a predictor for fatal VF. The phase statistics approach was first introduced by Wu et al. for the study of financial time series [48, 49]. The authors found that the approach can catch structure information of time series and is suitable for the analysis of wave profiles of VF ECG. The phase statistics analysis is in principle an extension of HHT, and is capable of describing morphologies of a wave in a statistical sense [16, 17]. The study of Wu et al. includes collections of ECG for SCD and VF from patients, and the signal analysis of the resultant VF ECG. In this section, we will shortly review their analysis by HHT. Again, details of the study and extended investigations which are not included herein will be referred to the original paper [16, 17].

ECG records the electric potential of myocardial cells at the body surface as a function of time, and the occurrence of VF signals implies the heart does not work (to pump blood) normally. More precisely, normal ECG explicitly shows P wave, QRS complexes, and T wave, while there is lack of QRS complexes wave form in VF ECG. Figure 16.6 shows the comparison between a typical normal ECG and VF ECG signal used in the study. Apparently, it is possible to extract the intervals of VF from ECG chart by technician by directly visual inspection. In this study, the ECG for SCD and VF by using a portable 24-hour Holter has been collected. The

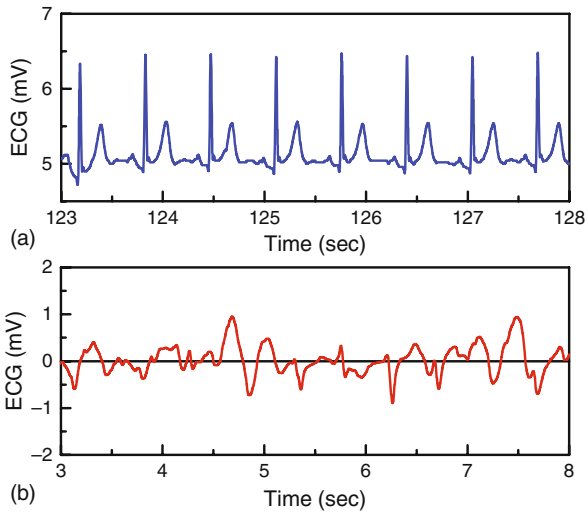

Fig. 16.6 (**a**) A typical normal ECG, and (**b**) VF ECG signal used in the study

data were recorded by the CM5 lead (the bipolar V5 lead) at a sampling frequency of 125 Hz. There were totally 24 patients involved in the study, but 7 of the patients did not suffer from the VF problem and data for one patient was not recorded. Among the remaining 16 subjects, there were 6 survivors and 10 non-survivors. The VF ECG segments were picked up by a medical doctor. Some patients have more than one VF ECG segment, and finally 27 VF ECG data were available for the analysis.

From the viewpoint of cellular eletrophysiology, the appearance of ventricular tachycardia is due to the formation of a reentrant wave in cardiac tissue, driving the ventricle at a rate much faster than the normal sinus rhythm. VF is a spatially and temporally disorganized state arising from the subsequent breakdown of the reentrant wave into multiple drifting and meandering spiral waves [50, 51]. Therefore, the detection of the characteristic features corresponding to the disordered state in ECG is likely a path toward the early evaluation of VF. In normal ECG, there are sharp P waves which are not suitable for direct analysis, while waveforms of VF ECG behave better and can be used for morphology analysis. Therefore, the analysis is only applied to the ECG data during VF.

The timing characteristics of transient features of nonstationary time series like VF ECG are best revealed using the concept of the instantaneous phase. The analysis is thus carried out by phase statistics. The phase statistics approach consists of the calculation of the instantaneous phase of a time series and the statistics of the calculated phases. In order faithfully to calculate the phase, we decompose empirical data into a number of well-defined IMFs by EMD, and calculate the instantaneous phase of resultant IMFs directly by the Hilbert transform. The phase statistics is achieved by defining the histogram of instantaneous phase satisfying the following normalization condition

$$\int P(\rho)d\rho = 1 \tag{16.15}$$

where $P(\cdots)$ stands for the probability density function (PDF). Direct calculations show that the PDF of instantaneous phase of the first IMF can be classified into three types of patterns, CV (convex), UF (uniform), and CC (concave), according to the morphologies of the histograms [17]. Furthermore, the statistics of 27 VF intervals and the best fit in the logistic regression concluded that the CV type VF is likely to be the fatal VF [17].

To quantify the phase distribution patterns, we define a measure χ,

$$\chi = \langle P_1(\phi_1)\rangle - \langle P_2(\phi_1)\rangle \tag{16.16}$$

where $\langle\cdots\rangle$ denotes an average, P_1 is the PDF of the instantaneous phase ϕ_1 of the first IMF in the range $-0.5\pi \le \phi_1 \le 0.5\pi$, and P_2 is for the phase in the ranges $-\pi \le \phi_1 < -0.5\pi$ and $0.5\pi < \phi_1 \le \pi$. More specifically, χ is a measure of the difference between the average of the PDFs of the phases located in the range $-0.5\pi \le \phi_1 \le 0.5\pi$ and the average of those not in this range. According to this definition, we have $\chi > \varepsilon$ for the CV type, $|\chi| \le \varepsilon$ for the UF type, and $\chi < -\varepsilon$

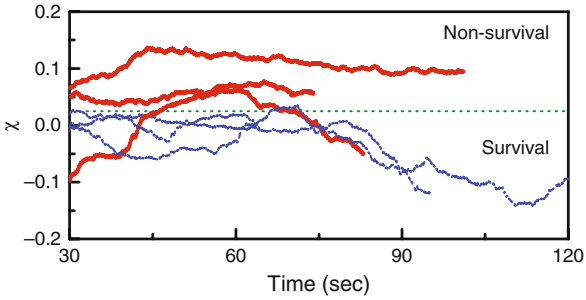

Fig. 16.7 χ as a function of time for typical VFs of survivals (*dashed line/blue color*) and non-survivals (*thick solid line/red color*). *Dotted line* is the threshold which separates regimes of survival and non-survival. After Ref. [16]

for the CC type. The value of ε is determined by the properties of statistics. It is better to establish a proper threshold of χ such that there is a clear separation for the CV type pattern from the UF and CC types. From the analysis of Holter data from 16 individuals, it was found that taking $\varepsilon = 0.025$ gives reasonable results which are consistent with direct visual inspection. Note that $\varepsilon = 0.025$ corresponds to a tolerance of 5% from the probability $P = 0.5$. Hence, one can describe the temporal evolution of the phase histogram by measuring $\chi(t)$ with a fixed window. As $\chi(t)$ enters into the regime of the CV type pattern $\chi(t) > \varepsilon$, it is considered as an indication of the occurrence of fatal VF. For practical purposes, here we take a window of 30 sec. Figure 16.7 shows χ as a function of time for typical VFs of three survivals and three non-survivals. The threshold ε of $\chi(t)$ can substantially separate the survival and non-survival groups into survival and non-survival regimes, and $\chi(t)$ for survivors rarely enter into the non-survival regime. As a result, the technique offers a new possibility to improve the effectiveness of intervention in defibrillation treatment and limit the negative side effects of unnecessary interventions. It can also be implemented in real time and should provide a useful method for early evaluation of fatal VF [16].

16.5 Conclusions

We have briefly explored the applications of HHT to biomedical data processing. The remarkable advantage of HHT in these applications is that it can catch primary structures of intrinsic rhythms from empirical data based on its adaptive feature [13, 17]. It should be pointed out that although intermittence test was used in this study, a more general method of EEMD [18] should be tested in the future. The EEMD enjoys an advantage of not setting the intermittence criterion subjectively.

In the study of CS, we found that from a physiological viewpoint, it is difficult to precisely identify the mechanisms responsible for the observed non-linear interactions in CS. However, cardiac oscillations are more regular than respiratory oscillations, and CS occurs at the period when respiratory signals become regular enough. Therefore, the regularity of respiratory signals contributes dominantly to the synchronization. Consequently, over-filtered signals may cause a misleading

conclusion that there is CS. The adaptivity of HHT allows us to effectively keep the signal structures and avoid the introduction of artificial periodicity easily appear in the Fourier-based filters with priori bases [13] and lead to a conclusion of too strong CS. From this aspect, HHT is better than other methods.

In the study of VF, we have used the phase statistics approach [48] to investigate ECG during VF in humans. In this approach, the HHT was used to calculate the instantaneous phase of IMFs decomposed from VF ECG, and the corresponding momentary phase histograms was then construct to inspect the evolution of the waveform of the time series. The HHT's capability of handling nonstationary and nonlinear time series allows us to define a measure as a monitor to inspect temporal evolution of the phase histogram of ECG during VF. The classification of VF ECG from the phase histograms further provides a possible route for early evaluation of fatal VF. Since to date there is no predictor available for fatal VF, this breakthrough may indicate the power and promise of HHT.

From the impressive achievements of the applications of HHT to CS and VF ECG time series analysis as presented in this article, we expect that HHT can also be applied to other biomedical data. Among others, the importance of biomedical image has been emphasized for a long time, and 2D HHT to biomedical imaging applications is promising. We are working this direction, and results will be reported in the near future.

Acknowledgments This work was supported by the National Science Council of the Republic of China (Taiwan) under Grant Nos. NSC 96-2112-M-008-021-MY3 (M.-C. Wu) and NSC 95-2119-M-008-031-MY3 (N. E. Huang).

References

1. Peng CK, Costa M, Goldbergr AL (2009) Adaptive Data Analysis of Complex Fluctuations in Physiologic Time Series. Adv Adapt Data Analy 1: 61–70
2. Huang NE, Shen Z, Long SR, Wu MC, Shin HH, Zheng Q, Yen NC, Tung CC, Liu HH (1998) The Empirical Mode Decomposition Method and the Hilbert Spectrum for Non-stationary Time Series Analysis. Proc Roy Soc London A 454: 903–995
3. Huang W, Shen Z, Huang NE, Fung YC (1998) Engineering analysis of biological variables: An example of blood pressure over 1 day. Proc Natl Acad Sci USA 95: 4816–4821
4. Huang W, Shen Z, Huang NE, Fung YC (1998) Engineering Analysis of Intrinsic Mode and Indicial Response in Biology: the Transient response of Pulmonary Blood Pressure to Step Hypoxia and Step Recovery. Proc Natl Acad Sci USA 95: 12766–12771
5. Huang W, Shen Z, Huang NE, Fung YC (1999) Nonlinear indicial response of complex nonstationary oscillations as pulmonary hypertension responding to step hypoxia. Proc Natl Acad Sci USA 96: 1834–1839
6. Cummings D, Irizarry R, Huang E, Endy T, Nisakak A, Ungchusak K, Burke D (2004) Travelling waves in dengue hemorrhagic fever incidence in Tailand. Nature 427: 344–347
7. Huang NE, Shen SSP (2005) edited. Hilbert-Huang Transform and Its Applications, World Scientific
8. Wu Z, Huang NE, Chen XY (2008) The 2 Dimensional Ensemble Empirical Mode Decomposition method, Patent (submitted)
9. Nunes JC, Bouaoune Y, Delechelle E, Niang O, Bunel P (2003) Image analysis by bidimensional empirical mode decomposition. Image Vis Comput 21: 1019–1026

10. Nunes JC, Guyot S, Deléchelle E (2005) Texture analysis based on local analysis of the bidimensional empirical mode decomposition. J Machine Vision Apply (MVA) 16: 177–188
11. Nunes JC, Deléchelle E (2009) Empirical Mode Decomposition: Applications on Signal and Image Processing. Adv Adapt Data Analy 1: 125–175
12. Yuan Y, Jin M, Song PJ, Zhang J (2009) Two dimensional empirical mode decomposition and dynamical detection of bottom topography with SAR picture. Adv Adapt Data Analy (in press)
13. Wu MC, Hu CK (2006) Empirical mode decomposition and synchrogram approach to cardiorespiratory synchronization. Phys Rev E 73: 051917
14. Wu MC (2007) Phase statistics approach to time series analysis. J Korean Phys Soc 50: 304–312
15. Wu MC (2007) Phase statistics approach to physiological and financial time series. AAPPS Bulletin 17: 21–26
16. Wu MC, Struzik ZR, Watanabe E, Yamamoto Y, Hu CK (2007) Temporal evolution for the phase histogram of ECG during human ventricular fibrillation. AIP Conf Proc 922: 573–576
17. Wu MC, Watanabe E, Struzki ZR, Hu CK, Yamamoto Y (2008) Fatal ventricular fibrillation can be identified by using phase statistics of human heart beat signals, submitted for publication
18. Wu Z, Huang NE (2009) Ensemble Empirical Mode Decomposition: A Noise Assisted Data Analysis Method. Adv Adapt Data Analy 1: 1–42
19. Tass P, Rosenblum MG, Weule J, Kurths J, Pikovsky A, Volkmann J, Schnitzler A, Freund HJ (1998) Detection of *n:m* Phase Locking from Noisy Data: Application to Magnetoencephalography. Phys Rev Lett 31: 3291
20. Guyton AC (1991) Text book of medical physiology. 8th ed (Saunders, Philadelphia)
21. Bernardi L, Salvucci F, Suardi R, Solda PL, Calciati A, Perlini S, Falcone C, Ricciardi L (1990) Evidence for an intrinsic mechanism regulating heart-rate-variability in the transplanted and the intact heart during submaximal dynamic exercise. Cardiovasc Res 24: 969–981
22. Almasi J, Schmitt OH (1974) Basic technology of voluntary cardiorespiratory synchronization in electrocardiology. IEEE Trans Biomed Eng 21: 264–273
23. Rosenblum MG, Pikovsky AS, Kurths J (2004) Synchronization approach to analysis of biological systems. Fluctuation and Noise Lett 4: L53–L62
24. Rosenblum MG, Pikovsky AS (2004) Controlling Synchronization in an Ensemble of Globally Coupled Oscillators. Phys Rev Lett 92: 114102
25. Schreiber T (2000) Measuring Information Transfer. Phys Rev Lett 85: 461
26. Paluš M, Stefanovska A (2003) Direction of coupling from phases of interacting oscillators: An information-theoretic approach. Phys Rev E 67: 055201(R)
27. Jamsek J, Stefanovska A, McClintock PVE (2004) Nonlinear cardio-respiratory interactions revealed by time-phase bispectral analysis. Phys Med Bio 49: 4407–4425
28. Richter M, Schreiber T, Kaplan DT (1998) Fetal ECG extraction with nonlinear state-space projections. IEEE Eng Med Biol Mag 45: 133–137
29. Hegger R, Kantz H, Schreiber T (1999) Practical implementation of nonlinear time series methods: The TISEAN package. Chaos 9: 413–435
30. Kantz H, Schreiber T (1998) Human EGG: nonlinear deterministic versus stochastic aspects. IEE Proc Sci Meas Technol 145: 279–284
31. Toledo E, Roseblum MG, Schäfer C, Kurhts J, Akselrod S (1998) Quantification of cardiorespiratory synchronization in normal and heart transplant subjects. In: Proc. of Int. Symposium on Nonlinear Theory and its Applications, vol.1. Lausanne: Presses polytechniques et universitaries romandes, 171–174
32. Schäfer C, Rosenblum MG, Kurths J, Abel HH (1998) Heartbeat synchronized with ventilation. Nature (London) 392: 239–240
33. Schäfer C, Rosenblum MG, Abel HH, Kurths J (1999) Synchronization in the human cardiorespiratory system. Phys Rev E 60: 857

34. Rosenblum MG, Kurths J, Pikovsky A, Schäfer C, Tass P, Abel HH (1998) Synchronization in noisy systems and cardiorespiratory interaction. IEEE Eng Med Biol Mag 17: 46–53
35. Toledo E, Rosenblum MG, Kurths J, Akselrod S (1999) Cardiorespiratory synchronization: is it a real phenomenon? In: Computers in Cardiology, vol. 26, Los Alamitos (CA), IEEE Computer Society, 237–240
36. Lotric MB, Stefanovska A (2000) Synchronization and modulation in the human cardiorespiratory system. Physica A 283: 451–461
37. Toledo E, Akselrod S, Pinhas I, Aravot D (2002) Does synchronization reflect a true interaction in the cardiorespiratory system? Med Eng Phys 24: 45–52
38. Mrowka R, Patzak A (2000) Quantitative analysis of cardiorespiratory synchronization in infants. Int J Bifur Chaos 10: 2479–2488
39. Stefanovska A, Haken H, McClintock PVE, Hozic M, Bajrovic F, Ribaric S (2000) Reversible Transitions between Synchronization States of the Cardiorespiratory System. Phys Rev Lett 85: 4831
40. Quiroga RQ, Arnhold J, Grassberger P (2000) Learning driver-response relationships from synchronization patterns. Phys Rev E 61: 5142
41. Quiroga RQ, Kraskov A, Kreuz T, Grassberger PP (2002) Performance of different synchronization measures in real data: A case study on electroencephalographic signals. Phys Rev E 65: 041903
42. Kotani K, Takamasu K, Ashkenazy Y, Stanley HE, Yamamoto Y (2002) Model for cardiorespiratory synchronization in humans. Phys Rev E 65: 051923
43. Rosenblum MG, Pikovsky AS, Kurths J (1996) Phase Synchronization of Chaotic Oscillators. Phys Rev Lett 76: 1804
44. Iyengar N, Peng CK, Morin R, Goldberger AL, Lipsitz LA (1996) Age-related alterations in the fractal scaling of cardiac interbeat interval dynamics. Am J Physiol 271: 1078–1084, Data sets are available from http://physionet.org/physiobank/database/fantasia/. The subject codes used in the article follow those in the database
45. Wu Z, Huang NE (2004) A study of the characteristics of white noise using the empirical mode decomposition method. Proc R Soc London A 460: 1597–1611
46. Flandrin P, Rilling G, Gonçalvès P (2004) Empirical mode decomposition as a filter bank. IEEE Signal Proc Lett 11: 112–114
47. Zipes DP, et al (2006) ACC/AHA/ESC 2006 guidelines for management of patients with ventricular arrhythmias and the prevention of sudden cardiac death: a report of the American College of Cardiology/American Heart Association Task Force and the European Society of Cardiology Committee for Practice Guidelines (Writing Committee to Develop Guidelines for Management of Patients with Ventricular Arrhythmias and the Prevention of Sudden Cardiac Death). Europace 8: 746
48. Wu MC, Huang MC, Yu HC, Chiang TC (2006) Phase distribution and phase correlation of financial time series. Phys Rev E 73: 016118
49. Wu MC (2007) Phase correlation of foreign exchange time series. Physica A 375: 633–642
50. Christini DJ, Glass L (2002) Introduction: Mapping and control of complex cardiac arrhythmias. Chaos 12: 732–739
51. Bursac N, Aguel F, Tung L (2004) Multiarm spirals in a two-dimensional cardiac substrate. Proc Natl Acad Sci USA 101: 15530–15534